BMC Immunology

RESEARCH

Open Access

Comparative efficacy of preventive vs. therapeutic resveratrol in modulating gut microbiota and alleviating inflammation in DSS-induced colitis

Senmei Qin[1†], Zongjing Yang[1†], Jinqing Lei[1], Qingli Xie[1], Linsui Jiang[1], Yuanyuan Fan[1], Yonggu Luo[1], Kecong Wei[2], Wei Luo[3*] and Bing Yu[4*]

Abstract

Background Inflammatory bowel disease (IBD) management remains challenging due to limited preventive strategies and the low bioavailability of therapeutic agents like resveratrol (RSV). While RSV exhibits anti-inflammatory properties, its preventive potential via gut microbiome modulation remains unexplored.

Methods A murine colitis model was established using 2.5% DSS, with mice randomized into control (CON), DSS, therapeutic RSV treatment (RSV), and preventive RSV treatment (PRE) groups. Clinical outcomes, intestinal barrier integrity, inflammatory cytokines, macrophage polarization, TLR4/NF-κB signaling, and gut microbiota (16S rRNA sequencing) were systematically evaluated.

Results Preventive RSV (PRE) outperformed therapeutic RSV across all metrics. PRE attenuated colitis severity by 51.4% (weight loss, $P<0.001$ vs. RSV) and restored mucosal architecture ($P=0.048$ vs. DSS). Mechanistically, PRE normalized barrier function via transcriptional (ZO-1: 56.7% of CON; Occludin: 14-fold induction vs. DSS) and protein-level recovery (ZO-1: 96.5% of CON, $P=0.02$), suppressed pro-inflammatory cytokines (TNF-α: 80.8%; IL-6: 69.9%; IL-18: >96%, $P<0.001$ vs. DSS), and promoted M2 macrophage polarization (CD206: 1.7-fold vs. CON, $P=0.02$) through TLR4/NF-κB inhibition (53% TLR4 reduction vs. 15% with RSV, $P<0.001$). Despite comparable α-diversity between RSV and PRE, PRE uniquely enriched barrier-protective taxa (*Lactococcus*, *Muribaculum*) and restored microbial amino acid biosynthesis. Crucially, PRE's efficacy despite low systemic bioavailability implicated microbiome-mediated "luminal priming" as its primary mechanism.

Conclusions This study redefines preventive RSV as a microbial ecosystem engineer that preemptively fortifies the gut against inflammation via microbiome-immune-metabolic crosstalk. By prioritizing ecological prevention over

[†]Senmei Qin and Zongjing Yang are co-first authors.

*Correspondence:
Wei Luo
luoweinew@sr.gxmu.edu.cn
Bing Yu
yubing@sr.gxmu.edu.cn

Full list of author information is available at the end of the article

symptom suppression, our findings offer a transformative "food as medicine" strategy for IBD, highlighting RSV's potential as a chronotherapeutic agent to reshape clinical paradigms.

Keywords Resveratrol, Inflammatory bowel disease, Gut microbiota, Macrophage polarization, TLR4/NF-κB pathway

Introduction

Inflammatory bowel disease (IBD) represents a growing global health burden, with sharply rising incidence in Eastern countries paralleling its persistent prevalence in Western populations [1]. Despite advances in therapies such as biologics and immunosuppressants, clinical management remains hampered by high costs, adverse effects, and therapeutic resistance [2], underscoring an urgent need for preventive strategies targeting upstream disease mechanisms. Emerging evidence positions the gut microbiota as a master regulator of IBD pathogenesis, where dysbiosis disrupts barrier integrity, amplifies mucosal inflammation, and perpetuates immune dysregulation [3, 4]. Notably, microbial imbalances in IBD patients correlate with diminished colonization resistance against pathobionts (e.g., *Turicibacter*, *Gemella*) and impaired metabolic functions critical for epithelial repair [5–7], suggesting microbiota modulation as a viable preventive avenue.

Dietary polyphenols, particularly resveratrol (RSV), have garnered attention for their dual capacity to attenuate inflammation and reshape microbial ecosystems [8]. RSV exerts pleiotropic effects in preclinical IBD models, restoring gut barrier function [9] and reversing DSS-induced dysbiosis [10]. However, existing studies predominantly focus on its therapeutic application during active colitis [11], overlooking its preventive potential. This gap is critical given RSV's paradoxical efficacy despite low systemic bioavailability (< 5 ng/mL) [12], implying luminal microbiota-mediated mechanisms may drive its benefits. We hypothesize that preventive RSV administration primes a resilient microbial community capable of preemptively counteracting inflammatory triggers—a concept we term "microbial priming."

This study systematically investigates RSV's preventive efficacy in DSS-induced colitis, contrasting preventive (PRE) versus therapeutic (RSV) regimens. Through multi-omics integration, we reveal that RSV orchestrates a protective network involving microbiota–epithelial crosstalk via barrier-enhancing taxa such as Lactococcus and Muribaculum, promotion of anti-inflammatory M2 macrophage polarization, and restoration of host metabolic pathways. Our findings redefine RSV as a microbial ecosystem engineer, offering a paradigm shift from symptom suppression to ecological prevention in IBD management.

Materials and methods

Experimental reagents

RSV was purchased from Tokyo Chemical Industry Co., Ltd. (TCI, Tokyo, Japan). The following primary antibodies were used in this study: ZO-1 (AF5145, Affinity Biosciences, Jiangsu, China), TLR4 (T61519, Abmart, Shanghai, China), Occludin (TD7504S, Solarbio, Beijing, China), phosphorylated NF-κB P65 (3033, Cell Signaling Technology, Danvers, USA), NF-κB P65 (bsm-33117 M, Bioss, Beijing, China), F4/80 (ab111101, Abcam, Cambridge, UK), iNOS (18985-1-AP, Proteintech, Wuhan, China), CD206 (YT5640, Immunoway, Jiangsu, China), and MYD88 (PA1779, Abmart, Shanghai, China). Dextran sulfate sodium (DSS, MW 36–50 kDa) was obtained from Yeasen Biotechnology (Shanghai, China).

Animal study

Eight-week-old male C57BL/6 mice (SPF grade, 20 ± 2 g) were purchased from the Experimental Animal Center of Guangxi Medical University. All mice were housed under standard laboratory conditions, maintained at 25 °C ± 3 °C with 53% ± 3% relative humidity and a 12-hour light/dark cycle. They had free access to food and water and were acclimated for 7 days prior to the experiment.

A total of 28 mice were randomly assigned to four groups ($n = 7$ per group): Control (CON), DSS-induced colitis model (DSS), therapeutic RSV treatment (RSV), and preventive RSV treatment (PRE). The therapeutic RSV dose was based on previous studies determining the optimal dosage [13, 14]. Mice in DSS received 5% carboxymethylcellulose (CMC) orally once daily from Day 1 to Day 14. Mice in RSV were treated with 100 mg/kg of RSV, suspended in 5% CMC, administered orally once daily from Day 1 to Day 14, starting at the time of DSS induction. The PRE received the same RSV dosage and vehicle, but the treatment began 7 days prior to DSS induction (from Day − 7 to Day 14).

To induce colitis, all mice in DSS, RSV, and PRE were given 2.5% DSS in drinking water from Day 1 to Day 7. Mice in CON was given water only, without DSS, RSV, or CMC treatment. On Day 14, after the final oral administration, all mice were fasted for 12 h with free access to water. Blood samples were then collected via orbital puncture, and the animals were euthanized by cervical dislocation. The entire colon, from the cecum to the rectum, was carefully dissected and measured. Colon tissues and fecal samples were collected and stored at − 80 °C for further analysis.

Blood stool fraction

Fecal occult blood was detected using a qualitative fecal occult blood test kit (Yuanye Bio-Technology, Shanghai,

Table 1 Disease activity index scoring criteria

Score	Weight loss (%)	Diarrheal stool	Blood
0	None	Normal	None
1	1–5	Soft but still formed	Thimbleful, blood steak
2	5–10	Soft and unformed	Modicum, blood clot
3	10–15	Loose	Visible bloody stools
4	>15	Diarrhea	Gross bleeding

China) based on the ortho-tolidine method [15]. Sample collection, processing, and testing were strictly performed according to the manufacturer's instructions.

Disease Activity Index (DAI) assessment

The DAI score was used to assess colitis severity, as described previously [16]: DAI was defined as the average of body weight loss score, fecal characteristics score and blood stool fraction and was used to evaluate the severity of colitis, and the items were listed in Table 1. DAI was calculated as following: DAI = (aggregate score of weight loss, stool consistency and bleeding) / 3.

Evaluating of spleen index

Mice spleens were harvested, cleaned of any surrounding tissue, and weighed after drying. The spleen index was calculated as follows: spleen index = spleen weight (mg) / body weight (g) [17].

Histopathologic evaluation of the colon

Colon tissues were fixed in 4% formalin in phosphate buffer for 24 h, then dehydrated, embedded in paraffin, and sectioned into 4 μm thick slices. Sections were stained with hematoxylin and eosin (H&E) using standard protocols. The tissue sections were examined using an ECLIPSE TS100 inverted microscope (Olympus Corporation, Japan). The inflammation score, based on inflammatory cell infiltration and tissue damage, was assessed as previously described [18].

Immunohistochemistry (IHC) staining analysis

Paraffin-embedded colon tissue sections (4 μm thick) were processed for IHC. Sections were incubated with the corresponding primary antibodies overnight at 4 °C, then incubated with secondary antibodies (enhanced enzyme-labelled goat anti-mouse/rabbit IgG polymer) for 30 min at room temperature according to the manufacturer's recommendations, and the expression of each indicator was detected by DAB chromatography. Brown staining was considered antibody positive. The tissue sections were examined using an ECLIPSE TS100 inverted microscope (Olympus Corporation, Japan). Positive areas were analysed by enabling Image J software to measure the average optical density of the brown areas.

RNA extraction and reverse transcription polymerase chain reaction assay

Total RNA was extracted using the TRIzol reagent (Takara, Japan) and reverse-transcribed into cDNA using the Takara reverse transcription kit. Real-time PCR was performed on a 7500 Real-Time PCR System (Applied Biosystems, USA). GAPDH was used as an internal control to normalize gene expression. Primer sequences for each target gene are listed in Table 2.

Western blot assay

Colonic tissues from mice were homogenized in ice-cold RIPA lysis buffer supplemented with PMSF and protease/phosphatase inhibitor cocktails (Solarbio, Beijing, China) according to the manufacturer's instructions. After sonication for complete protein extraction, the homogenates were centrifuged at 12,000 rpm for 15 min at 4 °C, and the supernatants were collected. Protein concentrations were determined using the BCA method(Biotechnology, Shanghai, China) [19]. Protein samples were mixed with 5× SDS-PAGE loading buffer at a 4:1 ratio and denatured by boiling at 100 °C for 10 min [20], Subsequently, 20–40 μg of protein was separated on 7.5-10%

Table 2 Primers of each gene

Target genes	Forward(5′-3′)	Reverse(5′-3′)
IL-18	GACTCTTGCGTCAACTTCAAGG	CAGGCTGTCTTTTGTCAACGA
IL-6	GAGAGGAGACTTCACAGAGGATACC	TCATTTCCACGATTTCCCAGAGAAC
TNF-α	ACGGCATGGATCTCAAAGACAACC	ATAGCAAATCGGCTGACGGTGTG
IL-10	CTTACTGACTGGCATGAGGATCA	GCAGCTCTAGGAGCATGTGG
Occludin	CTGGATCTATGTACGGCTCACA	TCCACGTAGAGACCAGTACCT
ZO-1	CGCCTCCTCCTCCTCCGTTG	CGCCCTTGGAATGTATGTGGAGAG
GAPDH	TGTGTCCGTCGTGGATCTGA	TTGCTGTTGAAGTCGCAGGAG
F4/80	TTCCTGCTGTGTCGTGCTGTTC	GCCGTCTGGTTGTCAGTCTTGTC
iNOS	CACCTTGTTCAGCTACGCCTTC	CTTGTCACCACCAGCAGTAGTTG
CD206	TGATTGGTGGCAATTCACGAGAGG	AACAGGCAGGGAAGGGTCAGTC
TLR4	TTCAGAACTTCAGTGGCTGG	TGTTAGTCCAGAGAAACTTCCT
MYD88	CTCGCAGTTTGTTGGATGCC	TCACGGTCTAACAAGGCCAG
NF-κB	TGCGATTCCGCTATAAATGCG	ACAAGTTCATGTGGATGAGGC

SDS-polyacrylamide gels (XNCM Biotech, Suzhou, China) and transferred onto PVDF membranes (Sigma-Aldrich, Germany). The membranes were blocked with 5% non-fat milk for 1 h at room temperature and then incubated with primary antibodies overnight at 4 °C. After washing, the membranes were incubated with HRP-conjugated secondary antibodies (Invitrogen; Goat anti-Rabbit IgG [H + L], SA5-35571, or Goat anti-Mouse IgG [H + L], SA5-35521; 1:10,000 dilution) for 1 h at room temperature with gentle shaking. Protein bands were visualized using the Odyssey Infrared Imaging System (LI-COR) and quantified using ImageJ software (NIH, USA) [21], with β-actin serving as the loading control. All experiments were performed with at least three biological replicates. Full-length blots are provided in Supplementary file.

16S rDNA sequencing

Fresh fecal samples were collected post-euthanasia from all experimental groups, immediately snap-frozen in liquid nitrogen, and stored at − 80 °C. DNA was extracted using the TD601 Soil Fecal Genomic DNA Extraction Kit (Tianmo Biotech, Beijing, China) following the manufacturer's protocol. Sequencing was performed by Genesky Biotechnologies Inc. (Shanghai, China).

16S rRNA gene amplification and sequencing

Multiple spike-ins with conserved regions identical to natural 16S rRNA genes and variable regions replaced by random sequences with approximately 40% GC content were artificially synthesized. An appropriate proportion of the spike-in mixture with known gradient copy numbers was added to the sample DNA. The V3–V4 hypervariable regions of the 16S rRNA gene, along with spike-ins, were amplified using primers 341F (5'-CCTACGGGGGCWGCAG-3') and 805R (5'-GACTACHAGGGGTATCTAATCC-3'), followed by paired-end sequencing on an Illumina PE250 platform.

Data processing and analysis Raw read sequences were processed in QIIME2. Adapter and primer sequences were trimmed using the cutadapt plugin. The DADA2 plugin was used for quality control and to identify amplicon sequence variants (ASVs). Taxonomic assignments of ASV representative sequences were performed with a confidence threshold of 0.8 by a pre-trained Naive Bayes classifier trained on the Greengenes database (version 13.8). Spike-in sequences were identified, and reads were counted. A standard curve for each sample was generated based on read-counts versus spike-in copy number, and the absolute copy number of each ASV in each sample was calculated using the read-counts of the corresponding ASV. Spike-in sequences, not being components of the sample flora, were removed in subsequent analyses [22].

Statistical analysis

All data are presented as mean ± standard deviation (mean ± SD). Statistical analyses were performed using GraphPad Prism version 9.5.0 (GraphPad Software, USA). The Shapiro-Wilk test was employed to assess data normality, while the Brown-Forsythe test was used to verify homogeneity of variances. For datasets satisfying both normality ($P > 0.05$) and homogeneity of variances ($P > 0.05$), one-way analysis of variance (ANOVA) followed by Tukey's multiple comparisons test was applied. When either assumption was violated ($P \leq 0.05$ for either test), the Kruskal-Wallis test with Dunn's post hoc correction for multiple comparisons was utilized. All tests were two-tailed, and $P < 0.05$ was considered statistically significant.

Results

Preventive RSV attenuates DSS-induced colitis severity

To investigate the effects of RSV on the progression of IBD, we established a colitis mouse model using 2.5% DSS solution (Fig. 1A). DSS administration induced characteristic colitis progression, with preventive RSV treatment (PRE) demonstrating chronotherapeutic superiority over therapeutic RSV treatment (RSV) in mitigating clinical and pathological manifestations.

As shown in Fig. 1B, C, administration of DSS showed significant weight loss ($P < 0.001$ vs. CON) and elevated DAI scores ($P < 0.001$ vs. CON). PRE significantly reduced body weight loss compared to RSV (51.4% attenuation; $P < 0.001$) and decreased DAI scores by 54.0% ($P < 0.001$ vs. RSV).

In Fig. 1D, E, colon length was significantly reduced in DSS (5.95 ± 0.13 cm) compared to CON (7.83 ± 0.46 cm, $P < 0.001$). However, PRE significantly restored colon length (7.41 ± 0.86 cm, $P = 0.004$ vs. DSS), reaching 94.6% of the control levels. RSV also increased colon length (6.79 ± 0.51 cm), corresponding to 86.7% of CON, but this difference was not statistically significant compared to DSS ($P = 0.14$). And Fig. 1F shows that administration of DSS significantly increased spleen index by 78.2% ($P < 0.001$ vs. CON). PRE reduced spleen index more effectively than RSV (1.4% greater reduction; $P = 0.002$ vs. DSS).

H&E staining (Fig. 1G-I) showed that DSS caused severe crypt damage, goblet cell depletion, and inflammatory infiltration. Both RSV and PRE reduced these pathological changes, with PRE exhibiting near-complete mucosal restoration. Histological scoring confirmed a significant improvement in PRE ($P = 0.048$ vs. DSS), while RSV showed only partial improvement ($P = 0.12$ vs. DSS).

These findings establish that preventive RSV administration provides comprehensive protection against colitis progression, exceeding the efficacy of post-onset therapeutic intervention.

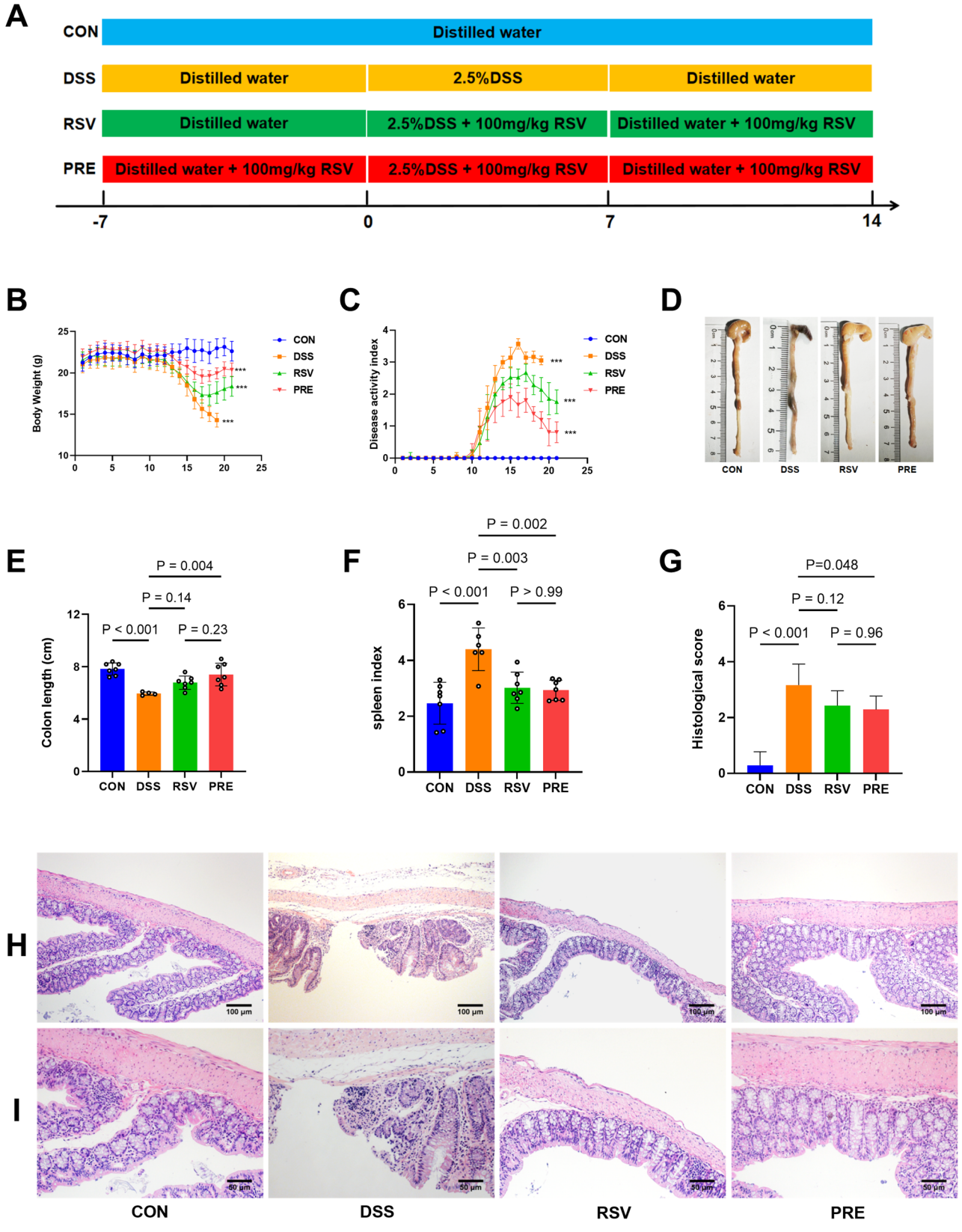

Fig. 1 (See legend on next page.)

(See figure on previous page.)

Fig. 1 Preventive RSV Treatment Mitigates DSS-Induced Colitis Severity. **A** Schematic diagram of the animal experimental design. **B** Body weight changes during the experiment. **C** DAI scores during the experiment. **D** Representative images of the colon. **E** Comparison of colon length in each group. **F** Comparison of spleen index in each group. **G** Histopathological scores in each group. **H**, **I** The representative images of H&E staining (magnification:100× and 200×, scale bar: 100 μm and 50 μm). Data are presented as mean ± SD, $n = 7$. $P < 0.05$ was considered statistically significant. CON, Control group, DSS, DSS-induced colitis model, RSV, therapeutic RSV treatment, PRE, preventive RSV treatment

Preventive RSV preserves intestinal barrier integrity

Intestinal barrier disruption is a hallmark of DSS-induced colitis, with tight junction proteins (TJs) playing a critical role in barrier integrity [23]. DSS-induced colonic barrier dysfunction was ameliorated by PRE, with distinct transcriptional, translational, and structural improvements.

As shown in Fig. 2A, B, administration of DSS significantly reduced mRNA levels of ZO-1 and Occludin by 62.0% ($P < 0.001$ vs. CON) and 87.0% ($P < 0.001$ vs. CON), respectively. While RSV partially restored Occludin expression ($P < 0.001$ vs. DSS), it had no effect on ZO-1 ($P = 0.94$ vs. DSS). PRE significantly increased ZO-1 expression to 56.7% of control levels ($P = 0.02$ vs. DSS) and upregulated Occludin expression by 14-fold compared to DSS ($P < 0.001$).

Western blot analysis (Fig. 2C-E) revealed that PRE restored ZO-1 protein to 96.5% of control levels ($P = 0.02$ vs. DSS), markedly outperforming RSV (59.7% of CON; $P = 0.34$). Occludin levels under PRE exceeded control values by 13.9% ($P = 0.001$). Immunohistochemical staining (Fig. 2F, G) demonstrated a 49.9% reduction in ZO-1 + junctional area in DSS-treated mice ($P = 0.002$ vs. CON), which was significantly restored by PRE ($P < 0.001$ vs. DSS; $P > 0.99$ vs. CON).

Compared to RSV, PRE showed superior efficacy in restoring barrier function: a 40.6% greater recovery of ZO-1 mRNA ($P = 0.04$), a 55.0% higher Occludin mRNA level ($P = 0.006$), and a 52.8% improvement in ZO-1 structural integrity ($P = 0.02$).

These results establish preventive RSV administration as a comprehensive strategy for intestinal barrier protection, combining molecular restitution with ultrastructural repair.

Preventive RSV restores inflammatory cytokine balance in DSS-induced colitis

Inflammatory cytokines play a critical role in the progression of IBD [24]. Figure 3A-D reveals that compared to CON, DSS administration significantly upregulated pro-inflammatory cytokines, including TNF-α ($P < 0.001$), IL-18 ($P < 0.001$), and IL-6 ($P < 0.001$), while showing a trend toward reduced IL-10 expression ($P = 0.06$). RSV significantly decreased IL-18 and IL-6 mRNA levels (both $P < 0.001$ vs. DSS) and increased IL-10 expression ($P = 0.02$ vs. DSS), but did not affect TNF-α mRNA levels ($P = 0.94$ vs. DSS). In contrast, PRE normalized TNF-α expression to near-control levels ($P = 0.17$ vs. CON), significantly suppressed pro-inflammatory cytokines (TNF-α: 80.8%; IL-6: 69.9%; IL-18: >96%, $P < 0.001$ vs. DSS), and increased IL-10 expression by 23.8-fold ($P < 0.001$ vs. DSS).

Compared to RSV, PRE exerted stronger effects on cytokine regulation, including a 77-percentage-point greater reduction in TNF-α mRNA ($P < 0.001$), a 2.7-fold higher induction of IL-10 ($P < 0.001$), and a more robust suppression of IL-18 (96.2% vs. 43.1%, $P < 0.001$).

These results establish that preventive RSV administration comprehensively restores cytokine homeostasis, outperforming therapeutic intervention in both pro-inflammatory suppression and anti-inflammatory restitution.

Preventive RSV promotes macrophage M2 polarization in DSS-induced colitis

Macrophages play a critical role in IBD pathogenesis [25]. DSS administration induced robust macrophage activation, characterized by an 18.9-fold upregulation of pan-macrophage marker F4/80 mRNA ($P < 0.001$ vs. CON) and an 9.13-fold increase in M1-polarization marker iNOS ($P = 0.002$ vs. CON). In contrast, M2-associated CD206 expression showed nonsignificant suppression ($P = 0.11$ vs. CON) (Fig. 4A-C).

RSV attenuated DSS-driven activation, reducing F4/80 ($P < 0.001$) and iNOS ($P = 0.01$) mRNA levels compared to DSS, but failed to restore CD206 mRNA expression ($P = 0.41$). PRE completely normalized iNOS to baseline levels ($P > 0.99$ vs. CON), elevated CD206 expression 1.7-fold above control ($P = 0.02$ vs. CON).

Immunohistochemical analysis supported these findings (Fig. 4D-G). DSS increased F4/80$^+$ macrophage infiltration by 1.2-fold compared to CON ($P = 0.10$). PRE restored macrophage density to near-physiological levels ($P = 0.01$ vs. DSS), outperforming RSV ($P = 0.05$ vs. DSS). Both treatments reduced iNOS$^+$ areas, with RSV and PRE achieving 35.1% ($P = 0.001$) and 38.7% ($P < 0.001$) reductions, respectively. CD206$^+$ cell recovery was observed only in PRE, showing a non-significant trend toward restoration ($P = 0.06$ vs. DSS).

These results establish preventive RSV administration as an effective strategy for macrophage phenotype modulation in colitis, with superior efficacy to post-onset therapeutic intervention.

Preventive RSV inhibits TLR4/NF-κB signaling in DSS-induced colitis

The TLR4/NF-κB pathway plays a crucial role in macrophage responses and inflammation [26]. As shown in Fig. 5A-C, compared to CON, administration of DSS significantly upregulated components of the TLR4/NF-κB pathway, including a 6.6-fold increase in TLR4 mRNA

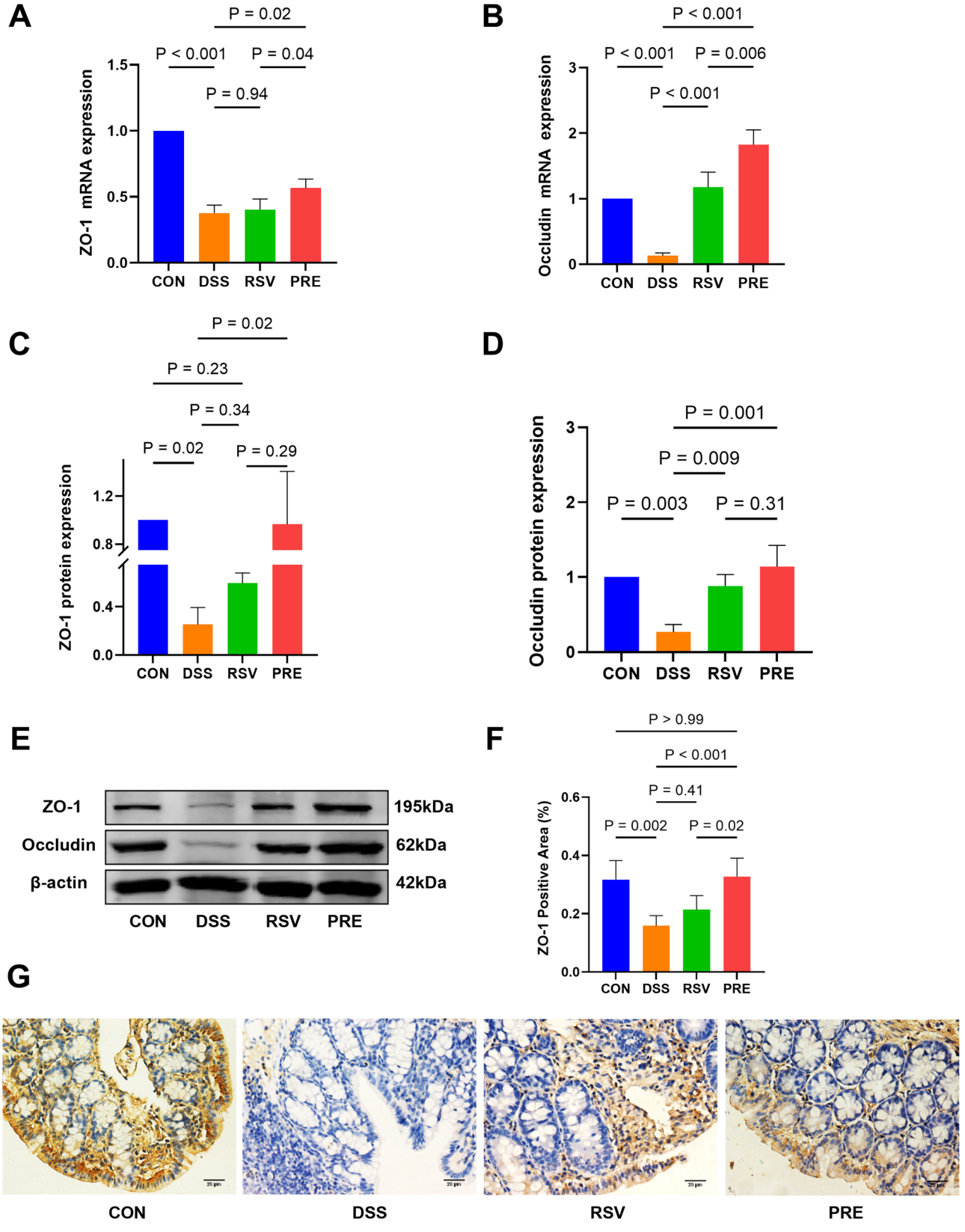

Fig. 2 (See legend on next page.)

(See figure on previous page.)

Fig. 2 Preventive RSV Treatment improves intestinal epithelial tight junction protein expression. **A**, **B** The relative mRNA expression levels of ZO-1 and Occludin in the colon tissue. **C**, **D** The expression ratios of ZO-1 and Occludin to β-actin. **E** Western blots of ZO-1, Occludin. **F**, **G** Immunohistochemical analysis of ZO-1 protein levels in mouse colon sections and representative images of immunohistochemical staining for ZO-1 (magnification: 400×, scale bar: 20 μm). Data are presented as mean ± SD, $n = 7$. $P < 0.05$ was considered statistically significant. CON, Control group, DSS, DSS-induced colitis model, RSV, therapeutic RSV treatment, PRE, preventive RSV treatment. Full-length blots are presented in Supplementary file

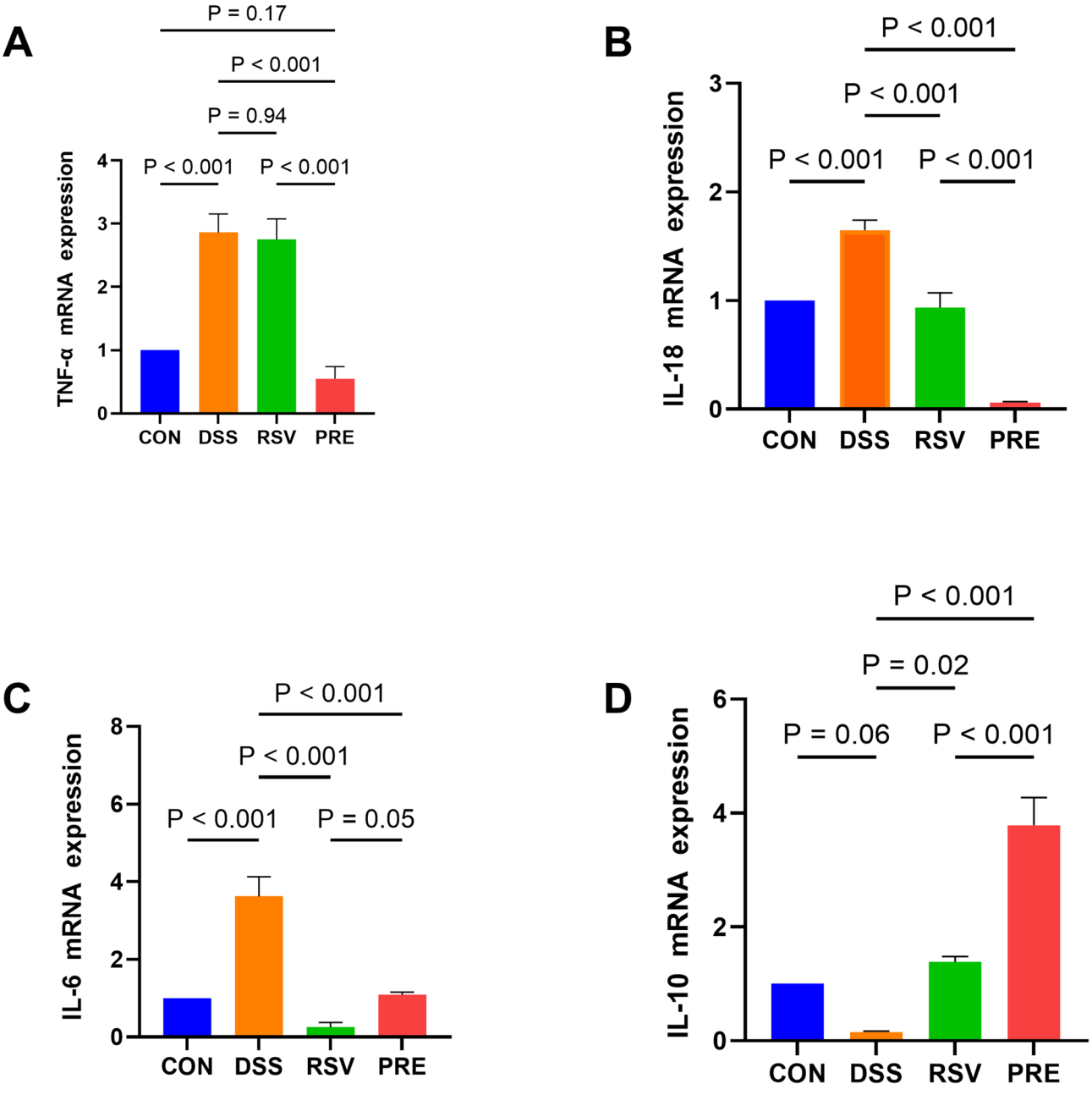

Fig. 3 Preventive RSV Treatment regulates the balance of inflammatory factors in DSS-induced colitis. **A**-**D** The relative mRNA expression levels of TNF-α, IL-18, IL-6, and IL-10 in the colon tissue. $n = 7$. $P < 0.05$ was considered statistically significant. CON, Control group, DSS, DSS-induced colitis model, RSV, therapeutic RSV treatment, PRE, preventive RSV treatment

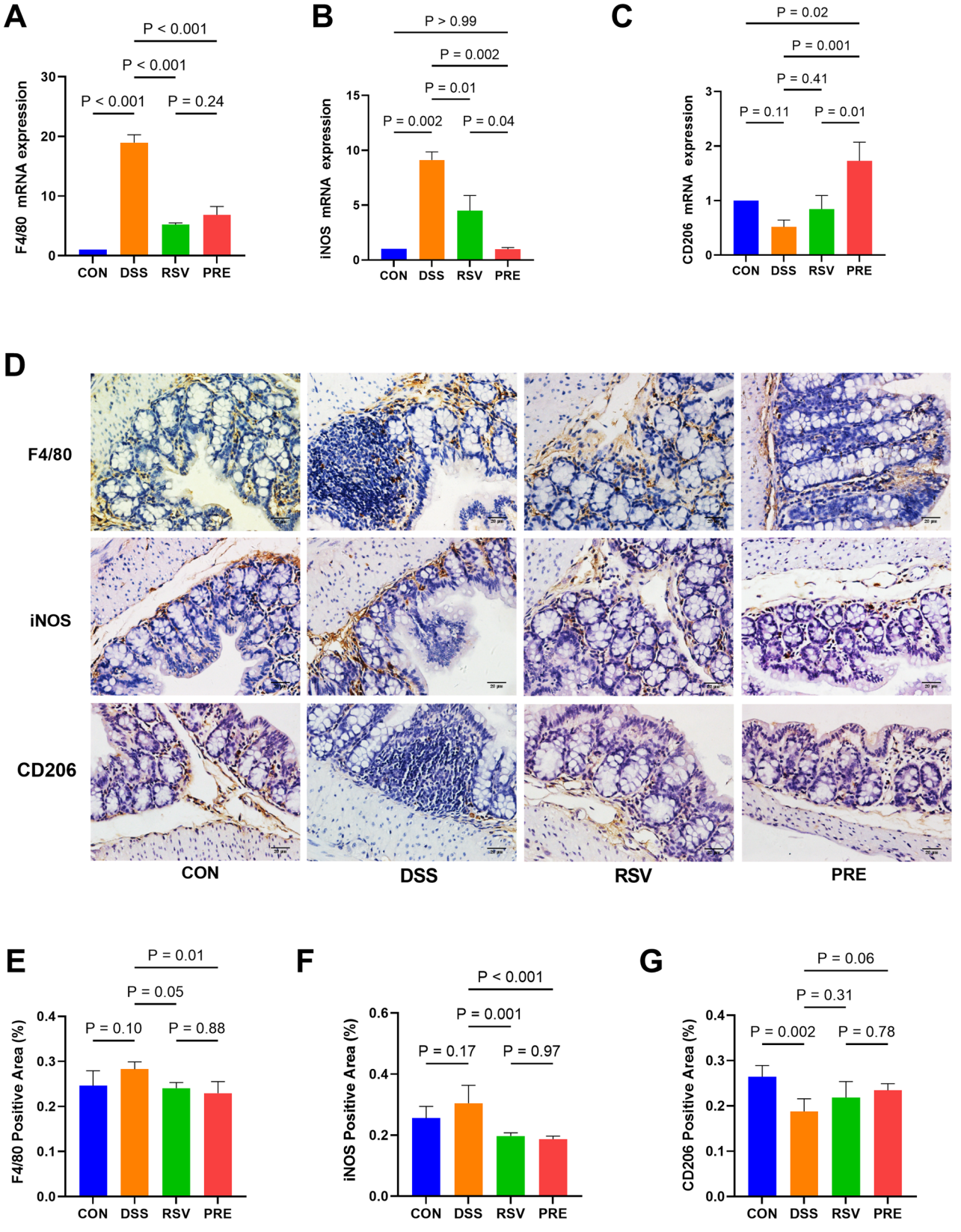

Fig. 4 Preventive RSV Treatment regulates the effect of DSS-induced macrophage M2 polarization in colitis. **A**-**C** The relative mRNA expression levels of F4/80, iNOS and CD206 in the colon tissue. **D**-**G** Representative images of immunohistochemical staining and immunohistochemical analysis of F4/80, iNOS, and CD206 protein levels in mouse colon sections (magnification: 400×, scale bar: 20 μm). Data are presented as mean ± SD, $n = 7$. $P < 0.05$ was considered statistically significant. CON, Control group, DSS, DSS-induced colitis model, RSV, therapeutic RSV treatment, PRE, preventive RSV treatment

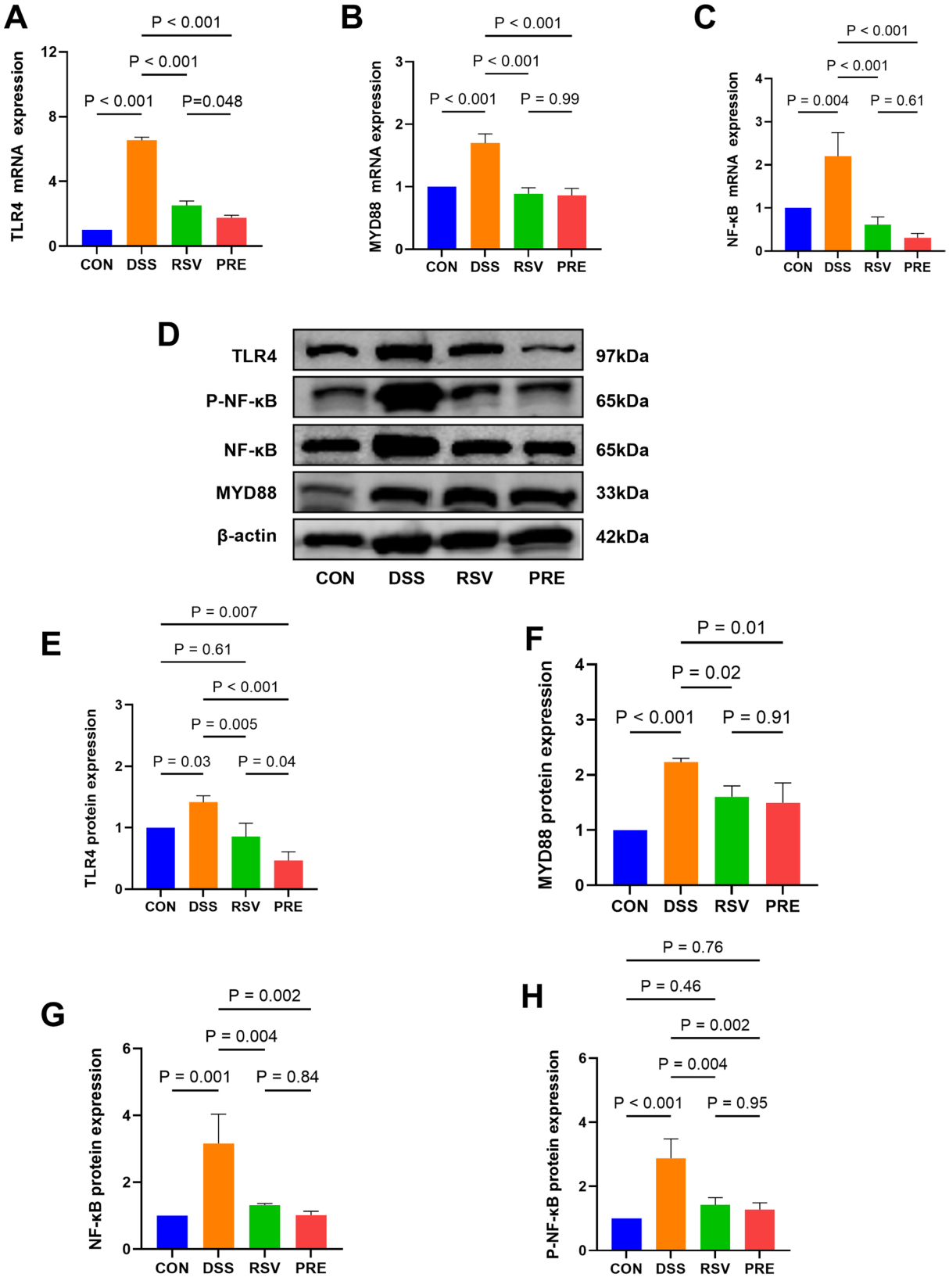

Fig. 5 Preventive RSV Treatment inhibites DSS-induced activation of the TLR4/NF-κB signaling pathway in colitis. **A**-**C** The relative mRNA expression levels of TLR4, MYD88 and NF-κB in the colon tissue. **D** Western blots of TLR4, P-NF-κB, NF-κB and MYD88. **E**-**H** The expression ratios of TLR4, MYD88, NF-κB and P-NF-κB to β-actin. Data are presented as mean ± SD, $n = 7$. $P < 0.05$ was considered statistically significant. CON, Control group, DSS, DSS-induced colitis model, RSV, therapeutic RSV treatment, PRE, preventive RSV treatment. Full-length blots are presented in Supplementary file

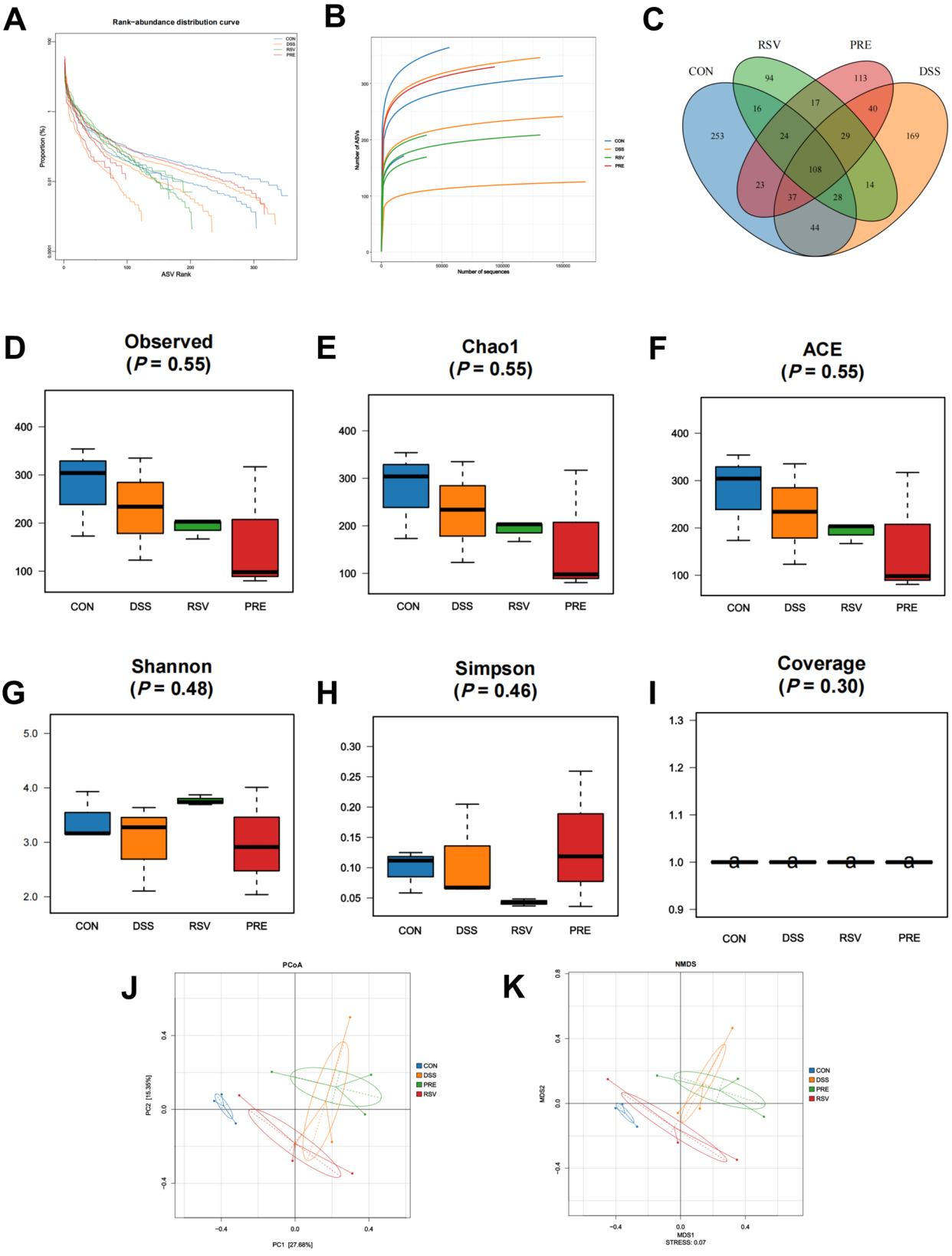

Fig. 6 (See legend on next page.)

(See figure on previous page.)

Fig. 6 Preventive RSV Treatment regulates changes in gut microbiota structure in mice with DSS-induced colitis. **A** Rank-abundance curves illustrating the distribution of species abundances within gut microbiota communities. **B** Rarefaction curves depicting the species richness across different gut microbiota groups. **C** Venn diagram highlighting the overlap and uniqueness of OTUs among different gut microbiota groups. **D**-**I** Gut microbial α-diversity analysis across experimental groups, including Observed, Chao1, ACE, Shannon, Simpson, and Coverage indices. **J** PCoA of gut microbiota composition across groups. **K** NMDS to explore the differences in gut microbiota structure between groups. Data are presented as mean ± SD, $n = 3$. $P < 0.05$ was considered statistically significant. CON, Control group, DSS, DSS-induced colitis model, RSV, therapeutic RSV treatment, PRE, preventive RSV treatment

transcription ($P < 0.001$), a 1.7-fold increase in MYD88 expression ($P < 0.001$), and a 2.2-fold induction of NF-κB ($P = 0.004$).

Both RSV and PRE significantly inhibited the expression of TLR4, MYD88, and NF-κB mRNA (all $P < 0.001$ vs. DSS). Furthermore, compared to RSV, PRE demonstrated a more pronounced inhibitory effect on TLR4 expression ($P = 0.048$).

Western blot analysis confirmed these findings at the protein level (Fig. 5D-H). PRE reduced TLR4 expression to 53% of control levels ($P = 0.007$), significantly outperforming RSV, which achieved only a 15% reduction ($P = 0.61$). Similarly, phospho-NF-κB levels were restored to baseline in PRE ($P = 0.76$ vs. CON), whereas RSV resulted in incomplete suppression ($P = 0.46$ vs. CON).

These findings collectively demonstrate that preventive RSV administration exerts multifaceted inhibition of the TLR4/NF-κB pathway, significantly surpassing therapeutic intervention in both efficacy and mechanistic scope.

RSV modulates the gut microbiota in DSS-induced colitis

Dysbiosis of the gut microbiota is strongly implicated in the pathogenesis of IBD [27]. To assess the impact of RSV on gut microbiota composition, we performed 16 S rRNA gene sequencing in DSS-induced colitis mice. Rank abundance (Fig. 6A) and rarefaction curves (Fig. 6B) confirmed stable sequencing with an adequate sample size. The Venn diagram (Fig. 6C) illustrates shared operational taxonomic units (OTUs) across the groups, with unique OTUs for each treatment: CON (253), DSS (169), RSV (94), and PRE (113). DSS mice exhibited reduced species richness compared to CON mice, with further reductions observed in RSV and PRE.

There were no significant differences in microbial richness and α-diversity (Observed, Chao1, ACE, Shannon, Simpson and Coverage indices) between CON, DSS, RSV, and PRE ($P > 0.05$) (Fig. 6D-I). PCoA (Fig. 6J) and NMDS (Fig. 6K) analysis revealed distinct microbiota compositions between DSS and CON, with the RSV and PRE clustering closer to CON.

At the phylum (Fig. 7A) and genus (Fig. 7B) levels, the microbiota composition varied across groups. Group-specific taxa were identified through LEfSe analysis and Linear Discriminant Analysis (LDA score > 2.0) (Fig. 7C, D). CON was enriched in *Lactobacillus* intestinalis, *Lactococcus*, and *Muribaculum*, while DSS was dominated by *Turicibacter*, *Staphylococcaceae*, and *Gemella*. In PRE, *Moraxellaceae* was the dominant taxa. Notably, no significant differences in dominant microbial taxa were observed between RSV and PRE, suggesting that both treatments similarly modulate the gut microbiota to alleviate IBD through microbial community regulation. Genus-level taxa with significant differences included *Lactococcus* (Fig. 7E), *Muribaculum* (Fig. 7F), *Lactiplantibacillus* (Fig. 7G) *Burkholderia-Caballeronia-Paraburkholderia* (Fig. 7H), and *Gemella* (Fig. 7I).

KEGG pathway analysis (Fig. 7J) revealed that DSS treatment led to decreased pathways related to amino acid biosynthesis, DNA replication, and protein synthesis, whereas pathways linked to cellular processes, signaling, and transcriptional regulation were upregulated. RSV reversed these changes, restoring pathway abundance to baseline levels.

Summary, RSV treatment in DSS-induced colitis mice modulates gut microbiota composition, showing a shift towards a microbiota profile similar to CON, with no significant differences between RSV and PRE, and a reversal of DSS-induced alterations in microbial taxa and metabolic pathways related to amino acid biosynthesis, DNA replication, and protein synthesis.

Discussion

This study introduces a novel preventive strategy where preventive administration of RSV reshapes the gut microbiome prior to the induction of colitis, establishing a resilient intestinal microenvironment that mitigates DSS-induced pathology through multiple mechanisms. Our findings demonstrate that RSV confers protection against colitis not only through its direct anti-inflammatory effects but, crucially, by preconditioning the microbiota. This discovery holds significant translational potential for the prevention of IBD [28].

The primary innovation of this work lies in establishing the preemptive efficacy of RSV through gut microbiome modulation. While previous studies have primarily focused on RSV's therapeutic anti-inflammatory effects during active colitis [29], we uniquely show that PRE leads to superior outcomes in mitigating DSS-induced colitis. Notably, these outcomes include a 51.4% reduction in weight loss, a 54.0% decrease in DAI, a 96.5% recovery of ZO-1 protein expression (compared to 59.7% with RSV), and comprehensive cytokine regulation (77% greater TNF-α suppression and 2.7-fold IL-10 induction). Moreover, we observed preferential M2 macrophage

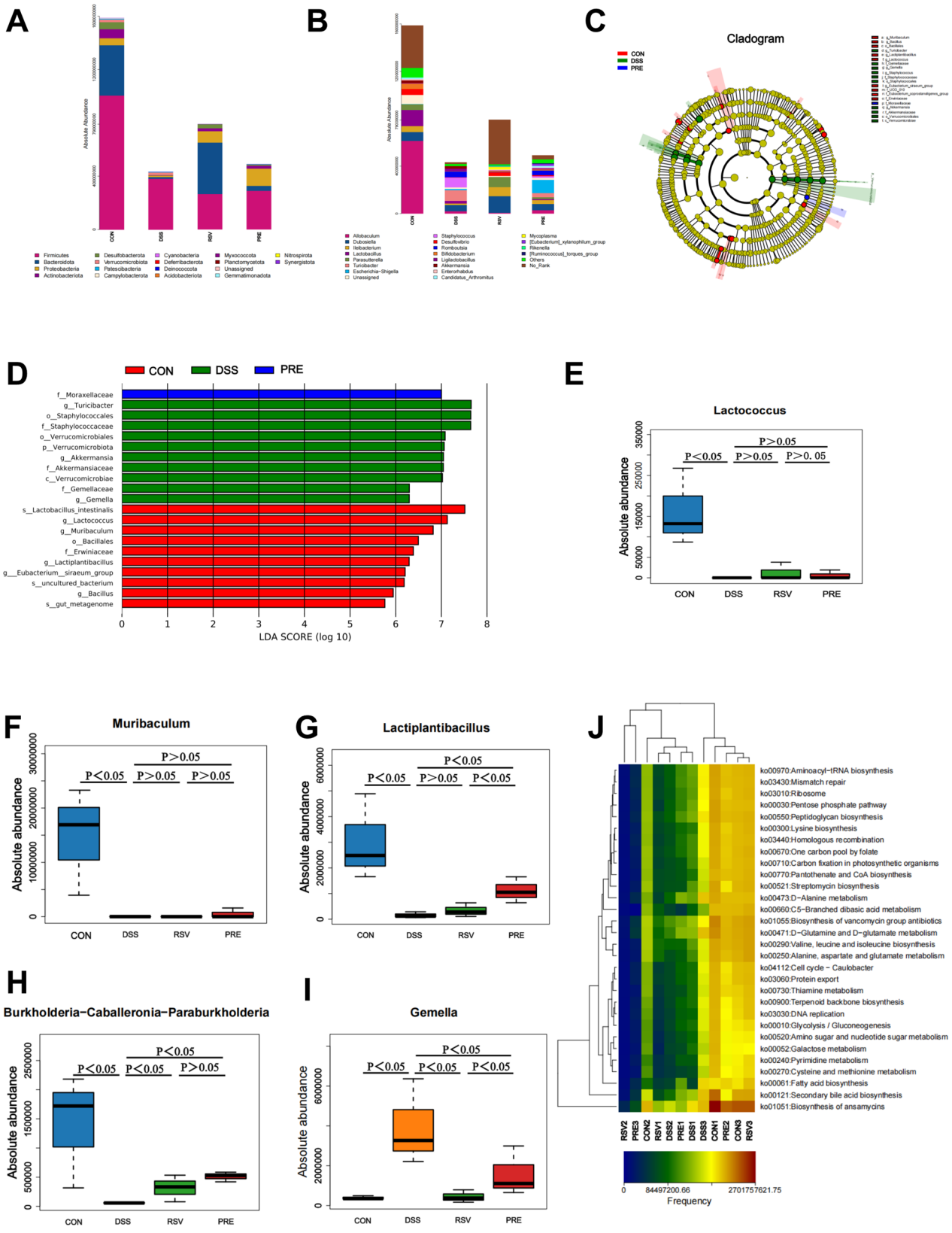

Fig. 7 (See legend on next page.)

(See figure on previous page.)

Fig. 7 Preventive RSV Treatment adjustes the compositional characteristics of the gut microbial community in DSS-induced colitis mice. **A**, **B** Relative abundance of microbial taxa at the phylum and genus levels. **C**, **D** Cladogram and LEfSe scores of biomarker screening. **E-I** Bar Charts of the Relative Abundance Distribution of Significantly Different Bacterial Genera. **J** Heatmap of KEGG functional pathway clustering. Data are presented as mean ± SD, $n = 3$. $P < 0.05$ was considered statistically significant. CON, Control, DSS, DSS-induced colitis model, RSV, therapeutic RSV treatment, PRE, preventive RSV treatment

polarization (1.7-fold CD206 elevation) and more potent inhibition of the TLR4/NF-κB pathway (53% reduction vs. 15% in RSV-treated mice). These results establish the PRE regimen as a preventive strategy with multifaceted mechanistic and functional benefits.

Importantly, no significant differences in the dominant microbial taxa between RSV and PRE were observed, suggesting that preventive RSV exerts its protective effects through modulation of the gut microbiome in DSS colitis mice. This implies that the microbiota's preconditioning precedes and potentiates RSV's anti-inflammatory effects, creating an intestinal environment that is resistant to inflammatory triggers—a concept we term "microbial priming".

Mechanistically, RSV orchestrates a tripartite protective network. Firstly, 16 S rRNA sequencing revealed that PRE specifically enriched barrier-enhancing *Lactococcus* and *Muribaculum* [30, 31], while suppressing pathobionts such as *Gemella* and *Turicibacter* [32, 33]. These microbial shifts correlated with earlier restoration of tight junctions, suggesting that microbiota-derived metabolites may accelerate epithelial repair. Secondly, PRE administration induced a 2.0-fold greater M2 macrophage polarization compared to RSV ($P = 0.01$), potentially via inhibition of the TLR4/NF-κB pathway (47% reduction in TLR4 for PRE vs. 15% for RSV) [34]. This "trained immunity" effect indicates that RSV preconditioning epigenetically primes myeloid cells toward an anti-inflammatory phenotype, enhancing immune tolerance and resilience. Thirdly, PICRUSt analysis revealed that PRE uniquely restored microbial amino acid biosynthesis, providing substrates for mucosal repair—a mechanism distinct from direct cytokine modulation. This suggests that RSV-enriched metabolites might directly contribute to epithelial repair by supplying essential nutrients for cellular regeneration [35].

Our data resolve the "RSV paradox" of its low bioavailability (serum < 5 ng/mL) yet high efficacy [12]. The PRE's enhanced outcomes, despite identical RSV dosing, suggest that microbiota-derived metabolites mediate protection, as evidenced by the correlation between restored microbial amino acid biosynthesis and enhanced ZO-1 expression [36]. This aligns with reports indicating that RSV-modulated gut microbes produce barrier-repairing metabolites such as indole-3-lactate [37]. These findings challenge the traditional pharmacokinetic paradigm, proposing that the luminal compartment may be the primary site of RSV's action.

However, several limitations should be addressed in future research. Although LEfSe analysis links Lactobacillus enrichment to protection, the lack of fecal microbiota transplantation (FMT) controls precludes definitive conclusions regarding microbial causality [38]. Additionally, the DSS model mimics acute colitis but does not fully capture the chronic and relapsing nature of IBD [39]. Future studies should employ chronic cycling models to assess the durability of RSV's protective effects over extended periods. Moreover, whether RSV inhibits TLR4/NF-κB signaling via direct receptor binding or through microbiota/macrophage crosstalk remains unclear. Spatial transcriptomics of TLR4-deficient macrophages in gnotobiotic models could help elucidate these mechanisms [40].

The translational implications of our findings are significant. The PRE's reduced DAI scores (54% reduction, $P < 0.001$ vs. RSV) support the development of RSV-enriched functional foods for IBD prevention. Notably, RSV achieved an 80.8% reduction in TNF-α levels (vs. DSS, $P < 0.001$) without inducing glucocorticoid-like adverse effects, aligning with reports suggesting that polyphenol-rich interventions can match conventional anti-TNF therapies in preclinical models [41]. As a natural compound found in common foods such as grapes, peanuts, and red wine, RSV holds promise as a potential "food-based" intervention with therapeutic applications in IBD prevention, highlighting its "food as medicine" potential.

Conclusion

This study redefines RSV as a microbial ecosystem engineer with chronotherapeutic potential. By preemptively reshaping microbial and immune responses, RSV prophylaxis creates a fortified intestinal niche that is resistant to inflammatory insults. This approach represents a paradigm shift from symptom management to ecological prevention in IBD.

Abbreviations

CMC	Carboxymethylcellulose
DSS	Dextran sulfate sodium
DAI	Disease Activity Index
Fig	Figure
H&E	Hematoxylin and Eosin
IBD	Inflammatory bowel disease
IHC	Immunohistochemistry
LDA	Linear Discriminant Analysis

OTUs Operational taxonomic units
TJs Tight junction proteins

Received: 21 March 2025 / Accepted: 6 May 2025
Published online: 28 May 2025

Supplementary Information

The online version contains supplementary material available at https://doi.org/10.1186/s12865-025-00718-3.

Supplementary Material 1.

Acknowledgements
Not applicable.

Authors' contributions
SMQ: Conceptualization, investigation, writing–original draft and editing. ZJY: Methodology, formal analysis, visualization, supervision, writing–review and editing. JQL: Investigation, validation, writing–review and editing. QLX: Data curation, software, project administration, writing–review and editing. LSJ: Conceptualization, writing–review and editing. YYF: Investigation, methodology, writing–review and editing. YGL: Resources, validation, project administration, writing–review and editing. KCW: Software, formal analysis, writing–review and editing. WL: Conceptualization, supervision, funding acquisition, project administration. BY: Methodology, formal analysis, resources, visualization, writing–review and editing.

Funding
This work was supported by the Natural Science Foundation of Guangxi Zhuang Autonomous Region (Grant No. 2023GXNSFAA026166, 2024GXNSFAA010132), the National Natural Science Foundation of China (Grant No. 82260109), and the Guangxi Zhuang Autonomous Region Administration of Traditional Chinese Medicine (Grant No. GXZYA20230264). The authors sincerely appreciate the financial support from these organizations.

Data availability
Sequence data that support the findings of this study have been deposited in NCBI Sequence Read Archive (SRA) with the primary accession code PRJNA1243306.

Declarations

Ethics approval and consent to participate
This study was approved by the Ethics Committee of the Second Affiliated Hospital of Guangxi Medical University (2022-KY(0791)) and conducted in accordance with the principles of the Declaration of Helsinki. All methods and experimental protocols adhered to the approved guidelines and ethical standards. Animal experiments were performed with the approval of the Institutional Animal Ethics Committee and complied with the institution's guidelines as well as the Regulations of the People's Republic of China on the Administration of Laboratory Animals, ensuring humane care and use of laboratory animals.

Consent for publication
Not applicable.

Competing interests
The authors declare no competing interests.

Author details
[1]Guangxi Medical University, Nanning 530021, Guangxi, China
[2]Department of Neurosurgery, Wuming Hospital of Guangxi Medical University, Wuming 530199, Guangxi, China
[3]Department of Gastroenterology, The First Affiliated Hospital of Guangxi Medical University, Nanning 530021, Guangxi, China
[4]Department of Gastroenterology, The Second Affiliated Hospital of Guangxi Medical University, Nanning 530007, Guangxi, China

References

1. Kamm MA. Rapid changes in epidemiology of inflammatory bowel disease. Lancet. 2017;390(10114):2741–42.
2. Burisch J, Zhao M, Odes S, De Cruz P, Vermeire S, Bernstein CN, Kaplan GG, Duricova D, Greenberg D, Melberg HO, et al. The cost of inflammatory bowel disease in high-income settings: a Lancet Gastroenterology Hepatology Commission. Lancet Gastroenterol Hepatol. 2023;8(5):458–92.
3. Zhu S, Han M, Liu S, Fan L, Shi H, Li P. Composition and diverse differences of intestinal microbiota in ulcerative colitis patients. Front Cell Infect Microbiol. 2022;12:953962.
4. Lee M, Chang EB. Inflammatory Bowel Diseases (IBD) and the microbiome-searching the crime scene for clues. Gastroenterology. 2021;160(2):524–37.
5. Ahlawat S, Kumar P, Mohan H, Goyal S, Sharma KK. Inflammatory bowel disease: tri-directional relationship between microbiota, immune system and intestinal epithelium. Crit Rev Microbiol. 2021;47(2):254–73.
6. Aldars-García L, Marin AC, Chaparro M, Gisbert JP. The interplay between immune system and microbiota in inflammatory bowel disease: a narrative review. Int J Mol Sci. 2021;22(6):3076.
7. Wu R, Xiong R, Li Y, Chen J, Yan R. Gut microbiome, metabolome, host immunity associated with inflammatory bowel disease and intervention of fecal microbiota transplantation. J Autoimmun. 2023;141:103062.
8. Yan J, Wang L, Gu Y, Hou H, Liu T, Ding Y, Cao H. Dietary patterns and gut microbiota changes in inflammatory bowel disease: current insights and future challenges. Nutrients. 2022;14(19):4003.
9. Alrafas HR, Busbee PB, Nagarkatti M, Nagarkatti PS. Resveratrol modulates the gut microbiota to prevent murine colitis development through induction of Tregs and suppression of Th17 cells. J Leukoc Biol. 2019;106(2):467–80.
10. Li F, Han Y, Cai X, Gu M, Sun J, Qi C, Goulette T, Song M, Li Z, Xiao H. Dietary resveratrol attenuated colitis and modulated gut microbiota in dextran sulfate sodium-treated mice. Food Funct. 2020;11(1):1063–73.
11. Yu B, Wang Y, Tan Z, Hong Z, Yao L, Huang S, Li Z, Zhang L, Li H. Resveratrol ameliorates DSS-induced ulcerative colitis by acting on mouse gut microbiota. Inflammopharmacology. 2024;32(3):2023–33.
12. Walle T, Hsieh F, DeLegge MH, Oatis JE Jr., Walle UK. High absorption but very low bioavailability of oral resveratrol in humans. Drug Metab Dispos. 2004;32(12):1377–82.
13. Yao J, Wei C, Wang JY, Zhang R, Li YX, Wang LS. Effect of resveratrol on Treg/Th17 signaling and ulcerative colitis treatment in mice. World J Gastroenterol. 2015;21(21):6572–81.
14. Singh UP, Singh NP, Singh B, Hofseth LJ, Taub DD, Price RL, Nagarkatti M, Nagarkatti PS. Role of resveratrol-induced CD11b(+) Gr-1(+) myeloid derived suppressor cells (MDSCs) in the reduction of CXCR3(+) T cells and amelioration of chronic colitis in IL-10(-/-) mice. Brain Behav Immun. 2012;26(1):72–82.
15. Jiang H, Shi GF, Fang YX, Liu YQ, Wang Q, Zheng X, Zhang DJ, Zhang J, Yin ZQ. Aloin A prevents ulcerative colitis in mice by enhancing the intestinal barrier function via suppressing the Notch signaling pathway. Phytomedicine. 2022;106:154403.
16. Xu Z, Chen W, Deng Q, Huang Q, Wang X, Yang C, Huang F. Flaxseed oligosaccharides alleviate DSS-induced colitis through modulation of gut microbiota and repair of the intestinal barrier in mice. Food Funct. 2020;11(9):8077–88.
17. Luo Y, Fu S, Liu Y, Kong S, Liao Q, Lin L, Li H. Banxia Xiexin decoction modulates gut microbiota and gut microbiota metabolism to alleviate DSS-induced ulcerative colitis. J Ethnopharmacol. 2024;326:117990.
18. Moallemian R, Rehman AU, Zhao N, Wang H, Chen H, Lin G, Ma X, Yu J. Immunoproteasome inhibitor DPLG3 attenuates experimental colitis by restraining NF-κB activation. Biochem Pharmacol. 2020;177:113964.
19. Liu K, Yin Y, Shi C, Yan C, Zhang Y, Qiu L, He S, Li G. Asiaticoside ameliorates DSS-induced colitis in mice by inhibiting inflammatory response, protecting intestinal barrier and regulating intestinal microecology. Phytother Res. 2024;38(4):2023–40.
20. Yu X, Li X, Xu Y, Li Y, Zhou Y, Zhang J, Guo L. Resveratrol ameliorates ulcerative colitis by upregulating Nrf2/HO–1 pathway activity: integrating animal experiments and network pharmacology. Mol Med Rep. 2024;29(5):77.
21. Cheng Z, Zhou Y, Xiong X, Li L, Chen Z, Wu F, Dong R, Liu Q, Zhao Y, Jiang S, et al. Traditional herbal pair Portulacae Herba and Granati Pericarpium alleviates DSS-induced colitis in mice through IL-6/STAT3/SOCS3 pathway. Phytomedicine. 2024;126:155283.

22. Gou Y, Cai S, Chen Y, Hou X, Zhang J, Bi C, Gu P, Yang M, Zhang H, Zhong W, et al. Atorvastatin improved ulcerative colitis in association with gut microbiota-derived tryptophan metabolism. Life Sci. 2024;351:122790.
23. Eichele DD, Kharbanda KK. Dextran sodium sulfate colitis murine model: an indispensable tool for advancing our understanding of inflammatory bowel diseases pathogenesis. World J Gastroenterol. 2017;23(33):6016–29.
24. Tian H, Wen Z, Liu Z, Guo Y, Liu G, Sun B. Comprehensive analysis of microbiome, metabolome and transcriptome revealed the mechanisms of Moringa oleifera polysaccharide on preventing ulcerative colitis. Int J Biol Macromol. 2022;222(Pt A):573–86.
25. Na YR, Stakenborg M, Seok SH, Matteoli G. Macrophages in intestinal inflammation and resolution: a potential therapeutic target in IBD. Nat Rev Gastroenterol Hepatol. 2019;16(9):531–43.
26. Yin J, Hu T, Xu L, Zhang L, Zhu J, Ye Y, Pang Z. Hsa_circRNA_103124 upregulation in Crohn's disease promoted macrophage M1 polarization to maintain an inflammatory microenvironment via activation of the AKT2 and TLR4/NF-κB pathways. Int Immunopharmacol. 2023;123:110763.
27. Shan Y, Lee M, Chang EB. The gut microbiome and inflammatory bowel diseases. Annu Rev Med. 2022;73:455–68.
28. Rudbaek JJ, Agrawal M, Torres, Mehandru S, Colombel JF, Jess T. Deciphering the different phases of preclinical inflammatory bowel disease. Nat Rev Gastroenterol Hepatol. 2024;21(2):86–100.
29. Lobo de Sá FD, Heimesaat MM, Bereswill S, Nattramilarasu PK, Schulzke JD, Bücker R. Resveratrol prevents campylobacter jejuni-induced leaky gut by restoring occludin and claudin-5 in the paracellular leak pathway. Front Pharmacol. 2021;12:640572.
30. Li H, Han L, Zong Y, Feng R, Chen W, Geng J, Li J, Zhao Y, Wang Y, He Z, et al. Deer oil improves ulcerative colitis induced by DSS in mice by regulating the intestinal microbiota and SCFAs metabolism and modulating NF-κB and Nrf2 signaling pathways. J Sci Food Agric. 2025;105(1):382–93.
31. Olate-Briones A, Albornoz-Muñoz S, Rodríguez-Arriaza F, Rodríguez-Vergara V, Aguirre JM, Liu C, Peña-Farfal C, Escobedo N, Herrada AA. Yerba Mate (Ilex paraguariensis) reduces colitis severity by promoting anti-inflammatory macrophage polarization. Nutrients. 2024;16(11):1616.
32. Rahman AT, Shin J, Whang CH, Jung W, Yoo D, Seo C, Cho BK, Jon S. Bilirubin nanomedicine rescues intestinal barrier destruction and restores mucosal immunity in colitis. ACS Nano. 2023;17(11):10996–1013.
33. Rengarajan S, Vivio EE, Parkes M, Peterson DA, Roberson EDO, Newberry RD, Ciorba MA, Hsieh CS. Dynamic immunoglobulin responses to gut bacteria during inflammatory bowel disease. Gut Microbes. 2020;11(3):405–20.
34. Dejban P, Nikravangolsefid N, Chamanara M, Dehpour A, Rashidian A. The role of medicinal products in the treatment of inflammatory bowel diseases (IBD) through inhibition of TLR4/NF-kappaB pathway. Phytother Res. 2021;35(2):835–45.
35. Zhou N, Wu N, Yao Y, Chen S, Xu M, Yin Z, Zhao Y, Tu Y. Anti-inflammatory effects of tripeptide WLS on TNF-α-induced HT-29 cells and DSS-induced colitis in mice. Food Funct. 2022;13(18):9496–512.
36. Cai J, Sun L, Gonzalez FJ. Gut microbiota-derived bile acids in intestinal immunity, inflammation, and tumorigenesis. Cell Host Microbe. 2022;30(3):289–300.
37. Cheng H, Zhang D, Wu J, Liu J, Zhou Y, Tan Y, Feng W, Peng C. Interactions between gut microbiota and polyphenols: a mechanistic and metabolomic review. Phytomedicine. 2023;119:154979.
38. Sheikh IA, Bianchi-Smak J, Laubitz D, Schiro G, Midura-Kiela MT, Besselsen DG, Vedantam G, Jarmakiewicz S, Filip R, Ghishan FK, et al. Transplant of microbiota from Crohn's disease patients to germ-free mice results in colitis. Gut Microbes. 2024;16(1):2333483.
39. Oh SY, Cho KA, Kang JL, Kim KH, Woo SY. Comparison of experimental mouse models of inflammatory bowel disease. Int J Mol Med. 2014;33(2):333–40.
40. Tian L, Chen F, Macosko EZ. The expanding vistas of spatial transcriptomics. Nat Biotechnol. 2023;41(6):773–82.
41. Yang W, Ma Y, Xu H, Zhu Z, Wu J, Xu C, Sun W, Zhao E, Wang M, Reis RL, et al. Mulberry biomass-derived nanomedicines mitigate colitis through improved inflamed mucosa accumulation and intestinal microenvironment modulation. Research (Wash D C). 2023;6:0188.

Publisher's Note